Determination of Creep Force, Moment, and Work Distribution in Rolling Contact With Slip

Bor-Tsuen Wang
Graduate Research Assistant.

Robert H. Fries
Associate Professor.

Department of Mechanical Engineering,
Virginia Polytechnic Institute
and State University,
Blacksburg, VA 24061

Investigators interested in the wear of wheels and rails frequently use a wear model that postulates wear is proportional to the work done in the contact patch. Most investigators compute the work using the rigid body motions of the wheel and the total creepage at the contact patch. Such an approach gives an overall or integrated measure of the wear in the contact patch. In previous wheel/rail wear work, we have assumed the wear to be distributed parabolically across the contact patch. In order to check this assumption and to permit refinement of our wear modeling technique, we desired to know the distribution of work within the contact patch. In order to compute the work distribution within the contact patch, we must be able to compute the distributions of both the creep force and the creepage. This paper describes a method of computing lateral and longitudinal creep force and creep moment distributions within the contact patch for combined rolling and slip conditions. It also describes the computations of creep distributions within the contact patch. The work distribution is computed from the dot product of force and creepage. The method uses Kalker's simplified theory to determine the force and creepage distributions. The actual computations are made using a modification of Kalker's program FASTSIM. A by-product of the work is the determination of the adhesion and slip regions for arbitrary creepage conditions.

Introduction

The problem of rolling contact with slip has been of high interest to rail vehicle dynamicists for a number of years. Tangential forces generated in the wheel/rail contact patch distinguish the dynamics of rail vehicles from the dynamics of other systems. Researchers in other fields have also been interested in the rolling contact problem. Rolling contact with slip can occur in machine elements including bearings, cams, and gears.

In most rail vehicle dynamics investigations, there is no particular interest in the distributions of tangential forces and moment in the contact patch. However, in wheel and rail wear predictions wherein wear is postulated to be proportional to the dot product of force and creepage, the distributions of force and creepage in the contact patch must be known in order to determine the distribution of wear in the contact patch.

In previous wheel/rail wear work (Fries and Davila, 1987), we have assumed the wear to be distributed parabolically across the contact patch. In order to check this assumption and to permit refinement of our wear modeling technique, we desired to know the distribution of work within the contact patch. In order to compute the work distribution within the contact patch, we must be able to compute the distributions of both the creep force and the creepage.

In later work we will use these results for wheel/rail wear predictions, and we will compare the wear predictions from the parabolic wear distribution model and the distribution obtained from the method described here.

In this work, we have made use of a FORTRAN program called FASTSIM (Kalker, 1982) to compute the creepage and force distributions. The wheel and rail are elastically similar for the case of steel wheels on steel rails. It is assumed that Coulomb friction conditions exist in the contact patch. Slip occurs when tangential forces are sufficient to overcome the friction force. Otherwise, the surfaces remain in contact without slip. Deformations are assumed to be elastic, and Hertzian contact stresses are assumed to exist in the contact patch. The normal contact stresses are computed first; then the tangential forces are computed. This implies an assumption that the normal contact stresses are uncoupled from the tangential stresses. We have additionally modified the FASTSIM code to compute the creep moment distribution in the contact patch.

A Brief Literature Review

The literature is rich with work on the rolling contact problem. A few of the more important contributions are summarized here. In one of the earliest contributions, Carter (1926) published a solution to the problem of two-dimensional rolling with slip. He considered the problem of traction between cylinders, and he included only longitudinal creepage.

Vermeulen and Johnson (1964) solved the rolling contact

Contributed by the Tribology Division for publication in the JOURNAL OF TRIBOLOGY. Manuscript received by the Tribology Division November 9, 1989.

problem for three-dimensional bodies in contact including both longitudinal and lateral creepage, but excluding spin creepage.

Kalker (1967a) took lateral creepage into account, and he obtained a simple approximate solution of the rolling contact problem. Later, he obtained a solution for the case of general creepage including spin (1967b). Kalker's linear theory, which assumes the existence of vanishingly small creepages and slip areas in the contact patch, provides the correct relationship between creepages and creep forces for small creepages. Because of its simplicity, linear theory has been widely adopted by researchers in rail vehicle dynamics.

More recently, Kalker (1982) developed a fast algorithm, called FASTSIM, that is based upon simplified theory. In Kalker's simplified theory, a linear relationship is assumed between the local traction and the local material elastic displacement. FASTSIM computes creep forces but not creep moment. In most rail vehicle work, the moment is relatively unimportant.

A number of rail vehicle dynamicists use a heuristic creep force model because of its simplicity and speed of computation. The heuristic model uses the creep coefficients from Kalker's (1967) linear theory, and the form of the creep force saturation curve from the Vermeulen and Johnson (1964) work. Shen et al. (1983) documented this model and compared its accuracy to computations based upon Kalker's FASTSIM algorithm and another algorithm called DUVOROL that was formulated by Kalker and Tjoeng (Shen et al., 1983).

Readers interested in more comprehensive information on solutions of the rolling contact problem are referred to a review paper by Kalker (1979) and books by Johnson (1985) and Garg and Dukkipati (1984).

Fries and Davila (1987) have given a brief review of the current wheel/rail wear literature. They discussed the issue of the contact patch work wear model and other contemporary models. A number of researchers have used the contact patch work model discussed here. Experimental evidence shows that this model provides a good macroscopic description of the wear process in some wear regimes.

The Wheel/Rail Rolling Contact Problem

Consider a wheel rolling over a rail at a nominal speed, V. The contact patch is an ellipse with the semiaxes a and b, according to Hertzian contact theory. The contact patch area is S. The normal contact pressure is P_z, and the shear tractions are P_X and P_Y. The creep forces and moment can be obtained by integrating the shear tractions over the contact area:

$$F_X = \iint_S P_X(x,y)dxdy \tag{1}$$

$$F_Y = \iint_S P_Y(x,y)dxdy \tag{2}$$

$$M_Z = \iint_S [P_Y(x,y)x - P_X(x,y)y]dxdy \tag{3}$$

where

F_X = longitudinal creep force
F_Y = lateral creep force
M_Z = creep moment
S = the region of the elliptical contact patch

$$S = \left\{(x,y)\left|\left(\frac{x}{a}\right)^2 + \left(\frac{y}{b}\right)^2 \le 1\right.\right\} \tag{4}$$

The creep forces depend upon the normal load, the creepages, the geometry of the contact bodies, and the coefficient of friction. Using Kalker's notation, we can express the Coulomb friction relationship as

$$(P_X, P_Y) \le \mu P_Z \tag{5}$$

where

μ = friction coefficient
P_Z = normal pressure
P_X, P_Y = longitudinal and lateral shear tractions

Creepages are normalized slip quantities. Longitudinal (ξ_X), lateral (ξ_Y), and spin (ξ_{SP}) creepages are defined as

$$\xi_X = \frac{V_{XW} - V_{XT}}{V} \tag{6}$$

$$\xi_Y = \frac{V_{YW} - V_{YT}}{V} \tag{7}$$

$$\xi_{SP} = \frac{\omega_{ZW} - \omega_{ZT}}{V} \tag{8}$$

where

V_{XW} = longitudinal velocity of wheel at the contact point
V_{XT} = longitudinal velocity of rail at the contact point
V_{YW} = lateral velocity of wheel at the contact point
V_{YT} = lateral velocity of rail at the contact point
ω_{ZW} = angular velocity of wheel at the contact point
ω_{ZT} = angular velocity of rail at the contact point
V = nominal velocity

Geometry and material properties of the contacting bodies affect the creep forces also. Since Hertzian contact conditions are assumed in this work, both bodies are assumed to be elastic and to possess constant curvatures in the contact region. The contact surface is assumed to be topographically smooth and clean.

In the work reported here, we have used a value of $\mu = 0.6$ for dry rolling contact. Other values can be used with equal ease.

Determination of Creep Force and Moment

The micro-slip velocity of the contact patch at position (x, y) between wheel and rail for steady rolling ($\partial\hat{u}_X/\partial t = 0$, $\partial\hat{u}_Y/\partial t = 0$) can be found from

$$W_X = (V_{XW} - V_{XT}) - (\omega_{ZW} - \omega_{ZT})y - V\left(\frac{\partial\hat{u}_{XW}}{\partial x} - \frac{\partial\hat{u}_{XT}}{\partial x}\right) \tag{9}$$

$$W_Y = (V_{YW} - V_{YT}) - (\omega_{ZW} - \omega_{ZT})x - V\left(\frac{\partial\hat{u}_{YW}}{\partial x} - \frac{\partial\hat{u}_{YT}}{\partial x}\right) \tag{10}$$

where

W_X, W_Y = micro-slip velocities of the particles at the surface of the contact patch
ω_{ZW} = spin angular velocity of wheel
ω_{ZT} = spin angular velocity of rail
$\hat{u}_{XW}, \hat{u}_{YW}$ = tangential elastic displacement of wheel
$\hat{u}_{XT}, \hat{u}_{YT}$ = tangential elastic displacement of rail

Dividing by the nominal velocity, V, and substituting the creepage definitions, equation (9) and (10) become

$$\frac{W_X}{V} = \xi_X - \xi_{SP}y - \frac{\partial u_X}{\partial x} \tag{11}$$

$$\frac{W_Y}{V} = \xi_Y - \xi_{SP}x - \frac{\partial u_Y}{\partial x} \tag{12}$$

where

V = nominal velocity
$u_X = \hat{u}_{XW} - \hat{u}_{XT}$
= difference of longitudinal elastic displacement of wheel and rail at (x, y) in contact patch coordinate

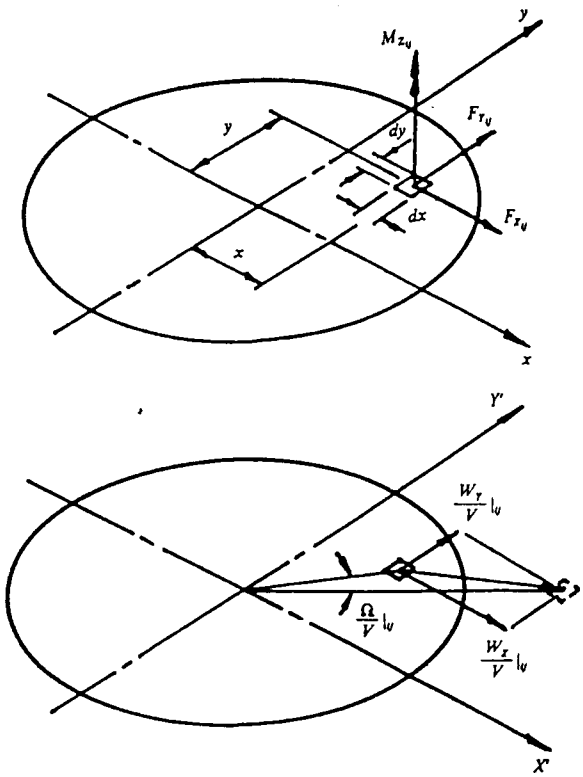

Fig. 1 Local creep forces and creepages

u_Y = $\hat{u}_{YW} - \hat{u}_{YT}$
= difference of lateral elastic displacement of wheel and rail at (x, y) in contact patch coordinate
ξ_X = longitudinal creepage
ξ_Y = lateral creepage
ξ_{SP} = spin creepage

Notice that W_X and W_Y include the rigid body motions consisting of translational motions in the x and y directions (ξ_X, ξ_Y), and rotational motion in the z direction $(\xi_{SP}y, \xi_{SP}x)$, and also elastic displacements $(\partial u_X/\partial x, \partial u_Y/\partial x)$.

In FASTSIM, Kalker (1982) nondimensionalized the variables for the implementation of the computation algorithm.

$$X' = \frac{x}{a} \qquad P'_X = \frac{P_X}{\mu Z_0}$$

$$Y' = \frac{x}{b} \qquad P'_Y = \frac{P_Y}{\mu Z_0}$$

$$Z' = \frac{P_Z}{Z_0} \tag{13}$$

$$Z_0 = \frac{N}{abP'} \tag{14}$$

$$N = \iint_S P_Z dxdy \tag{15}$$

$$P' = \iint_{S'} Z'dX'dY' = \iint_{S'} (1 - X'^2 - Y'^2)dX'dY' = \frac{\pi}{2} \tag{16}$$

$$S' = \{(X', Y') | X'^2 + Y'^2 \le 1\} \tag{17}$$

where

N = normal force
$(.\ .)'$ = the nondimensional quantities

Substitution of the above nondimensional quantities into the slip equations, (11) and (12), gives

$$W'_X = \xi'_X - Y'\xi'_{SP_X} - \frac{\partial P'_X}{\partial X'} \tag{18}$$

$$W'_Y = \xi'_Y - Y'\xi'_{SP_Y} - \frac{\partial P'_Y}{\partial X'} \tag{19}$$

where

$$W'_X = \frac{aW_{X1}}{\mu Z_0 V L_1} \tag{20}$$

$$W'_Y = \frac{aW_{Y1}}{\mu Z_0 V L_2} \tag{21}$$

$$\xi'_X = \frac{a\xi_X}{\mu Z_0 L_1} \tag{22}$$

$$\xi'_Y = \frac{a\xi_Y}{\mu Z_0 L_2} \tag{23}$$

$$\xi'_{SP_X} = \frac{ab\xi_{SP}}{\mu Z_0 L_3} \tag{24}$$

$$\xi'_{SP_Y} = \frac{a^2\xi_{SP}}{\mu Z_0 L_3} \tag{25}$$

L_1, L_2, and L_3 are derived from Kalker's linear theory. Kalker's (1982) paper describing FASTSIM contains expressions for L_1, L_2, and L_3. The normalized forces and moment can be obtained from

$$F'_X \equiv \iint_{S'} P'_X(X', Y')dX'dY' \tag{26}$$

$$F'_Y \equiv \iint_{S'} P'_Y(X', Y')dX'dY' \tag{27}$$

$$M'_Z \equiv \iint_{S'} \{P'_Y(X', Y')aX' - P'_X(X', Y')bY'\}dX'dY' \tag{28}$$

FASTSIM (Kalker, 1982) used equation (26) and (27) and the nondimensionalized quantities described above to compute the nondimensionalized lateral and longitudinal creep forces. We added equation (28) to the FASTSIM code to compute the nondimensionalized spin moment. Note that M'_Z in equation (28) is different from the nondimensionalized moment used by Kalker (1967c). The dimensional forces and moment are computed by

$$F_X = \frac{2}{\pi} N\mu F'_X \tag{29}$$

$$F_Y = \frac{2}{\pi} N\mu F'_Y \tag{30}$$

$$M_Z = \frac{2}{\pi} N\mu M'_Z \tag{31}$$

In addition to the resultant creep forces, F_X and F_Y, creep moment, M_Z, the local creep forces and moment at each subarea, $(F_{X_{ij}})$, $(F_{Y_{ij}})$, $(M_{Z_{ij}})$, and the local normalized slips $(W_X/V|_{ij})$, and $(W_Y/V|_{ij})$, and spin $(\Omega/V|_{ij})$ shown in Fig. 1 are computed by the modified FASTSIM.

Study of Slip and Adhesion Regions

The contact patch is divided into slip and adhesion regions. No relative motion occurs between the contacting bodies in the adhesion region. From Coulomb's law, the slip and adhesion regions are given by

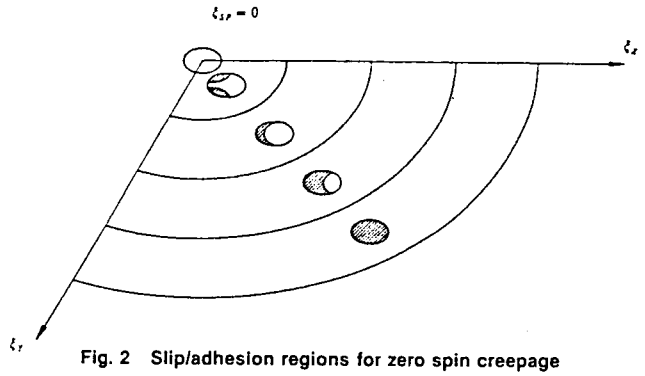

Fig. 2 Slip/adhesion regions for zero spin creepage

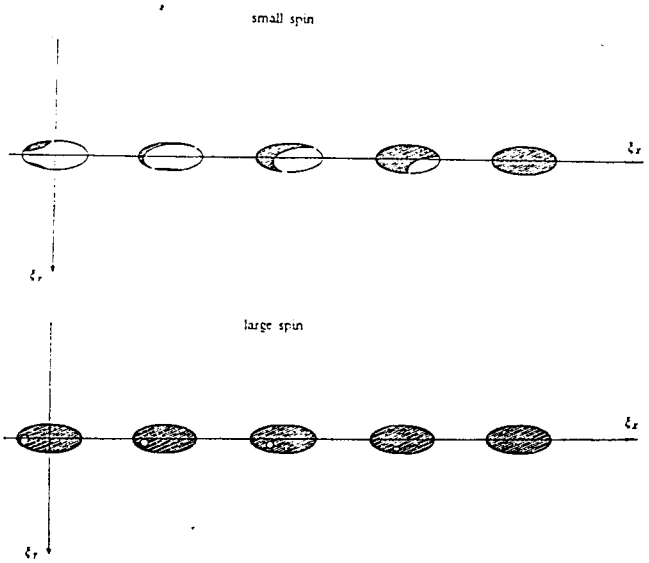

Fig. 3 Slip/adhesion regions for zero lateral creepage

$$S_{slip} = \{ (x,y) \mid (P_X(x,y), P_Y(x,y)) > \mu P_Z \} \quad (32)$$

$$S_{adh} = \{ (x,y) \mid (P_X(x,y), P_Y(x,y)) \leq \mu P_Z \} \quad (33)$$

where

S_{slip} = slip region
S_{adh} = adhesion region

The slip and adhesion regions are easily found using equations (32) and (33).

A number of factors affect the size and the distribution of the slip and adhesion regions. When the load, the geometry and material of the contacting bodies, and the coefficient of friction are fixed, then the influence of creepage alone on the slip and adhesion regions can be observed. For wear work, the locations of the slip and adhesion regions are important because no energy is dissipated in the adhesion region.

Figure 2 shows the distribution of slip and adhesion in a contact patch with $a/b = 2$. The slip region is crosshatched, the adhesion region is clear, and rolling is in the x-direction. The spin creepage is zero for Fig. 2. When the lateral and longitudinal creepages are increased, the slip region maintains symmetry with respect to the x-axis. With increased creepage, the slip region moves forward in the contact patch until the creepages are high enough that the slip region encompasses the entire region.

Figure 3 shows the distribution of slip and adhesion for the same conditions as Fig. 2 except that the lateral creepage is zero, and cases of small and large spin creepage are shown. The presence of spin creepage causes asymmetry of the slip and adhesion regions. The large spin case has sufficient spin creepage that the slip region nearly covers the contact patch.

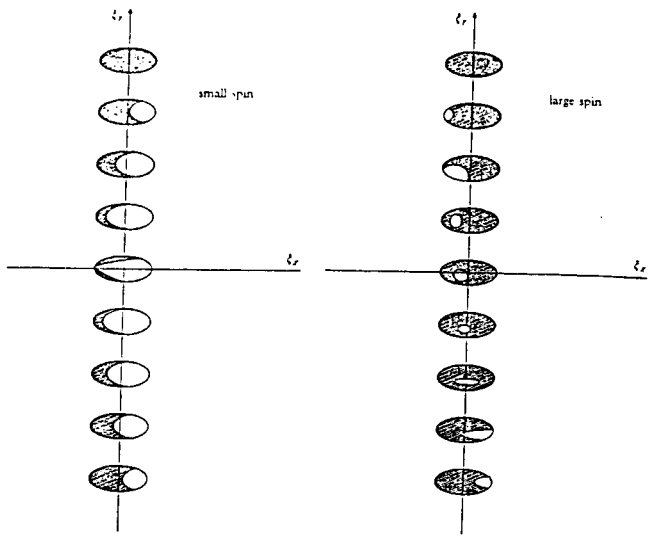

Fig. 4 Slip/adhesion regions for zero longitudinal creepage

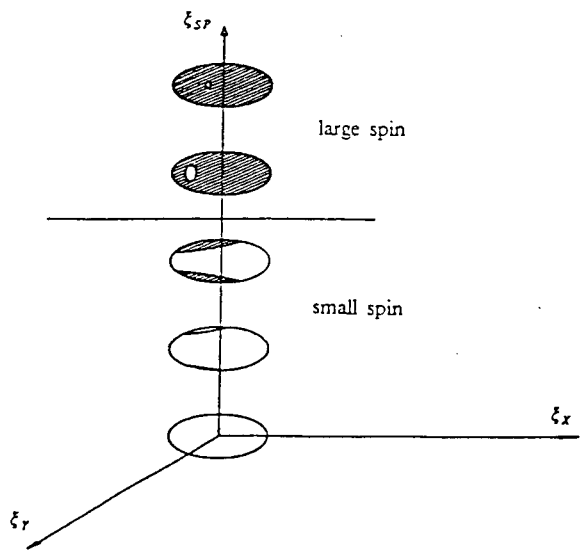

Fig. 5 Slip/adhesion regions for pure spin creepage

For small spin, the slip region is thicker on the negative side of the y-axis.

Figure 4 shows the distribution of slip and adhesion for the same conditions as Fig. 2 except that the longitudinal creepage is zero, and cases of small and large spin creepage are shown. For small spin creepage, the development of slip region is similar to the pure creepage case. For large spin creepage, only a small region of adhesion exists. This adhesion region migrates around the contact patch depending on the amount of lateral creepage present. It is at the trailing end of the contact patch for large lateral creepage, and at the leading edge of the contact patch for large negative lateral creepage.

Figure 5 shows the distribution of slip and adhesion for the same conditions as Fig. 2 except that the longitudinal and lateral creepages are zero. The slip and adhesion regions are symmetrical with respect to the x-axis for all cases in Fig. 5. For the small spin creepage case, the slip regions are at the edges of the contact patch. For the large spin creepage case, only a small region of adhesion exists. This adhesion region becomes progressively smaller as the spin creepage increases.

Distribution of Friction Work in the Contact Patch

The contact patch work can be computed in two ways. The global point of view considers the wheel as a rigid body. From

this point of view, the work done at the contact patch is the dot product of the creep force vector and the creepage vector multiplied by the contact patch velocity and time interval under consideration. Alternatively, the contact patch work can be computed by integrating all of the local work done over the entire contact patch. This second method accounts for the distribution of work done in the contact patch.

Global Work Determination. The global or macroscopic work done at the contact patch can be expressed as

$$(W_{\text{done}})_k = \{(F_X)_k(\xi_X)_k + (F_Y)_k(\xi_Y)_k + (M_Z)_k(\xi_{SP})_k\} V\Delta t \tag{34}$$

$$W_{\text{done lmacro}} = \sum_{k=1}^{N_t} (W_{\text{done}})_k = V\Delta t \sum_{k=1}^{N_t} \{(F_X)_k(\xi_X)_k + (F_Y)_k(\xi_Y)_k + (M_Z)_k(\xi_{SP})_k\} \tag{35}$$

where

$W_{\text{done lmacro}}$ = global work done over a time period, T
N_t = number of time intervals
Δt = time interval
$(W_{\text{done}})_k$ = global work done at time t_k
$(\ldots)_k$ = some quantity at time t_k

Local Work Determination. The creep forces and moment and the slip and spin creepages at each subarea of the contact patch are known, so the work done at each subarea of the contact patch can be computed and summed. The work expression is

$$(W_{\text{done}_{ij}})_k = V\Delta t\left\{(F_{X_{ij}})_k\left(\frac{W_X}{V}\Big|_{ij}\right)_k + (F_{Y_{ij}})_k\left(\frac{W_Y}{V}\Big|_{ij}\right)_k + (M_{Z_{ij}})_k\left(\frac{\Omega}{V}\Big|_{ij}\right)_k\right\} \tag{36}$$

where

$(W_{\text{done}_{ij}})_k$ = work done at subarea (x_i, y_j) in contact patch coordinate at time t_k

$\left(\frac{W_X}{V}\Big|_{ij}\right)_k$ = normalized longitudinal slip at subarea (x_i, y_i) in contact patch coordinate at time t_k

$\left(\frac{W_Y}{V}\Big|_{ij}\right)_k$ = normalized lateral slip at subarea (x_i, y_j) in contact patch coordinate at time t_k

$\left(\frac{\Omega}{V}\Big|_{ij}\right)_k$ = normalized spin at subarea (x_i, y_j) in contact patch coordinate at time t_k

$(F_{X_{ij}})_k$ = longitudinal creep force at subarea (x_i, y_j) in contact patch coordinate at time t_k

$(F_{Y_{ij}})_k$ = lateral creep force at subarea (x_i, y_j) in contact patch coordinate at time t_k

$(M_{Z_{ij}})_k$ = creep moment at subarea (x_i, y_j) in contact patch coordinate at time t_k

$$W_{\text{done lmicro}} = \sum_{k=1}^{N_t}\sum_{i=1}^{N_X}\sum_{j=1}^{N_Y}\{(W_{\text{done}_{ij}})_k\} \tag{37}$$

where

N_X = number of the subdivision of the contact patch along X-direction
N_Y = number of the subdivision of the contact patch along Y-direction

Comparison of Global and Local Work Quantities. Theoretically,

$$W_{\text{done lmacro}} = W_{\text{done lmicro}} \tag{38}$$

Actually, because of the contact patch discretization, a discrepancy exists between the macroscopic and microscopic work quantities. Although the difference is unavoidable, the distribution of work done at the contact patch appears to be reliable. By taking the macroscopic quantity to be correct, the previous equation can be revised to account for the difference between the macroscopic and the microscopic quantities. The microscopic work is multiplied by a factor, K, which is determined from the ratio of the macroscopic and microscopic works as shown below.

$$W_{\text{done lmacro}} = K \cdot W_{\text{done lmicro}} \tag{39}$$

where

K = a value that varies from case to case

In all cases that we have investigated, K is greater that 1.0. Table 1 gives values of K that are typical for several creepage conditions. The general trend is that K tends toward 1.0 when the creepage is large. For partial-slip cases, and for full-slip cases when the creepage is smaller, then K is larger than 1.0. For very small creepage, only a few of the discrete regions enter into the work computation, and K tends to be large.

Table 1 Values of K for several slip conditions

ξ_X	ξ_Y	ξ_{SP}	K	Slip condition
0.050	0.050	0.1	1.001	full slip
0.050	0.010	0.1	1.008	full slip
0.010	0.010	0.1	1.031	full slip
0.100	0.100	0.1	1.003	full slip
0.000	0.0022	0.576	1.424	full slip
0.0019	0.0011	0.144	1.602	partial slip
0.001	0.001	0.1	2.397	partial slip

Typical Results

Comparison of creep forces and moments obtained with the modified FASTSIM code with results in Kalker's (1967c) data book showed that differences are typically less than five percent. Larger differences occurred when the spin creepage was very large. Comparison between FASTSIM results and linear theory for small creepages were also usually within five percent. See Shen et al. (1983) for a more comprehensive comparison of creep force magnitude computed by various methods.

In order to visualize the distributions of creep force, moment, slip and work done at the contact patch, we plotted these quantities on 3-dimensional plots. Figures 6 and 7 show two typical cases. In these figures, the regions of slip and adhesion are shown in the upper left plot. The letter *s* indicates a region of slip, so the direction of the contact patch velocity vector is to the left. The upper right plot shows the contact patch work distribution. The remaining plots show the local creep force and creepage distributions within the contact patch.

The slip region shown in Fig. 6 results from positive longitudinal, lateral, and spin creepages. The creepages selected for Fig. 6 came from a tangent track simulation of a freight vehicle with three-piece trucks. These creepages are

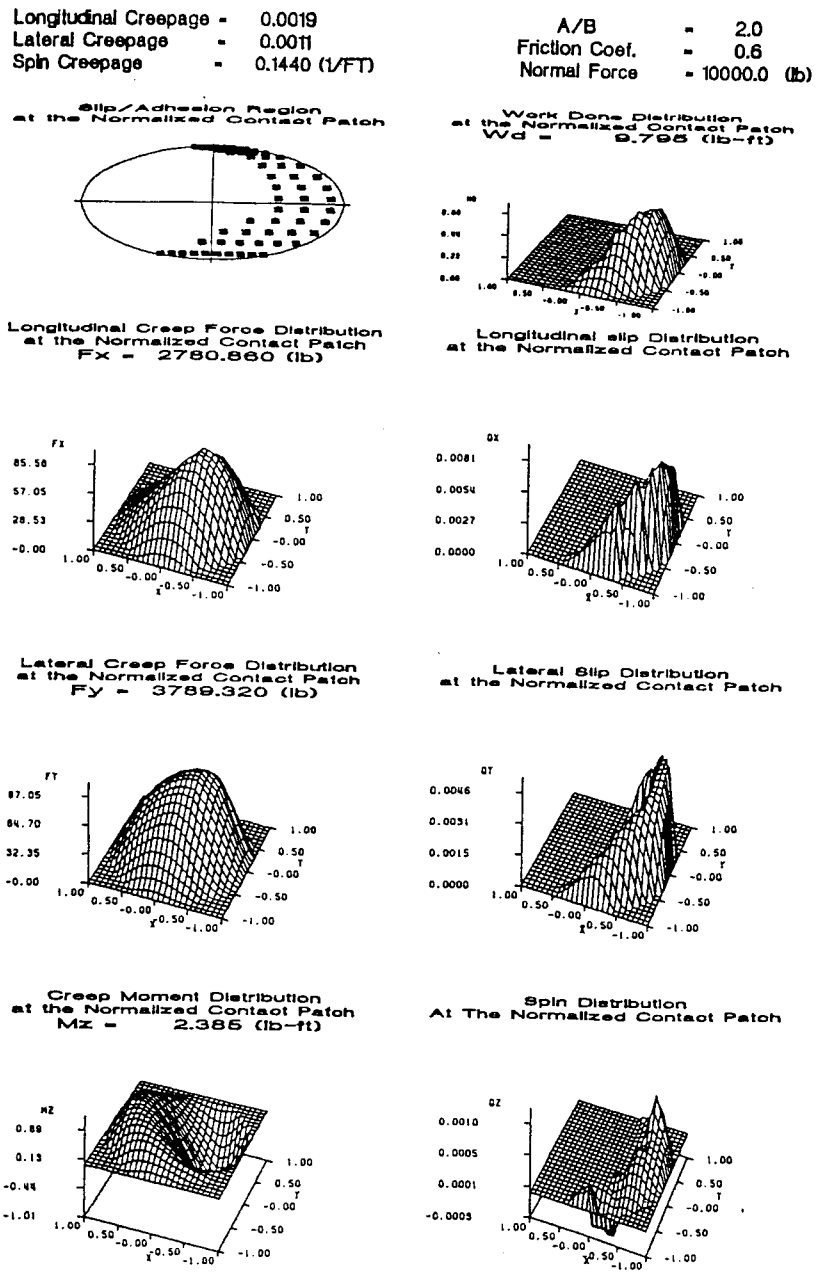

Fig. 6 Creep force, creepage, and work distributions for partial slip example

typical for tangent track running. The slip region covers the trailing portion of the contact patch. The work is zero in the adhesion region and positive in the slip region, as expected. The longitudinal and lateral forces are about 2800 and 3800 lb, respectively, and the spin moment is about 2 ft-lb. Obviously, the net contribution of the spin moment is small, but the spin creepage causes the slip region to be asymmetrical as shown.

Figure 7 shows results of a case with longitudinal creepage equal to zero. The lateral and spin creepages are sufficiently high to cause slip in the entire contact patch. The longitudinal and lateral creep forces are 0 and about 3300 lb, respectively, and the spin moment is about 9 ft-lb. Even though the net longitudinal force is zero, the longitudinal force distribution is not zero, as shown in the figure.

The primary motivation for this work was to compute the distributions of the creep force and creepage in the contact patch for use in wear predictions. Since we have previously assumed a parabolic distribution of work across the contact patch (Fries and Davila, 1987), we were interested in comparing the distributions obtained here to parabolic distributions. To make these comparisons, we integrated the distributions in Figs. 6 and 7 along the x-axis to obtain distributions of contact patch work in the lateral direction. Then we plotted these curves on the same axes as parabolas of about the same areas. Figure 8 shows the comparison for the Fig. 6 case, and Fig. 9 shows the comparison for the Fig. 7 case. Obviously, the distributions are quite different, and the parabolic wear distribution assumption is not justified. However, wheel wear profiles predicted using the parabolic wear distribution assumption are quite like those predicted using the method described in this paper (Wang, 1988). Comparisons between predicted wheel wear profiles and service-worn profiles also agree well for cases of tread wear and mild flange contact (Wang, 1988).

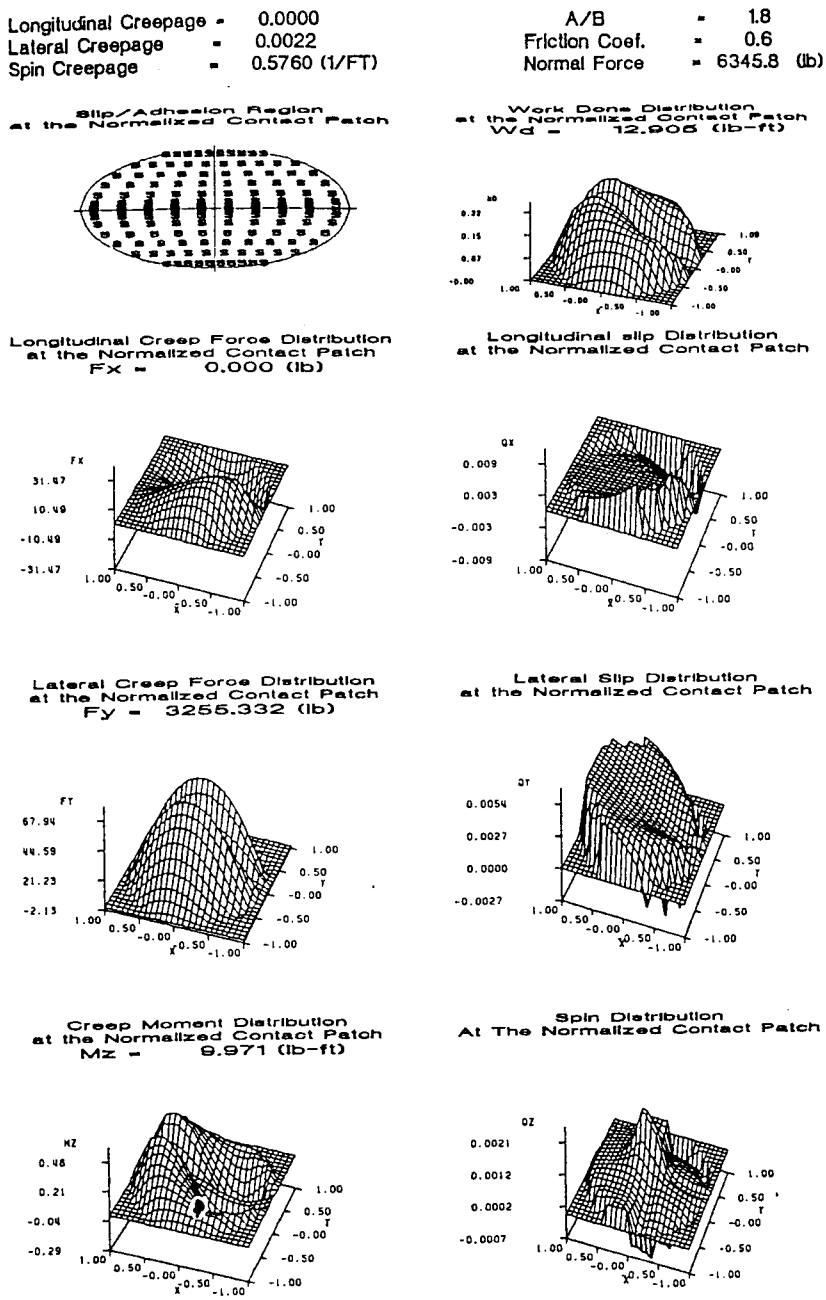

Fig. 7 Creep force, creepage, and work distributions for full slip example

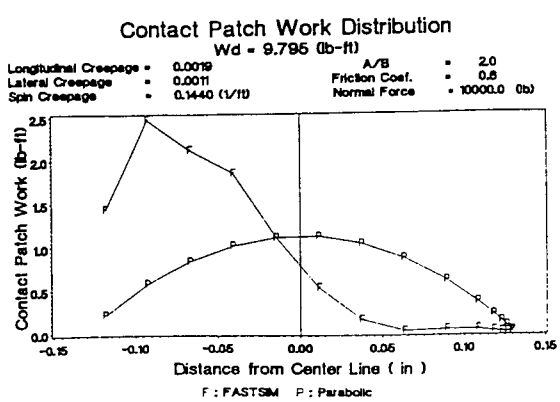

Fig. 8 Comparison of work distributions for partial slip example

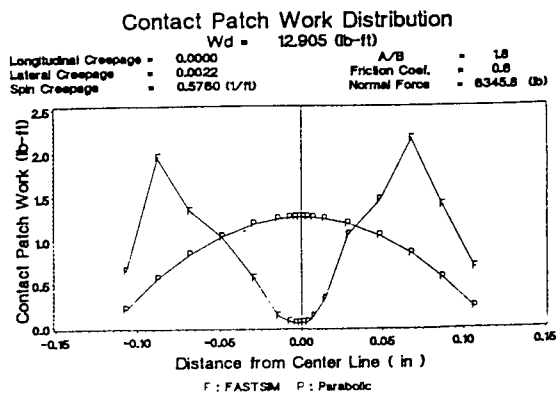

Fig. 9 Comparison of work distributions for full slip example

Summary and Conclusions

Kalker's program, FASTSIM, has been used to obtain the force, slip, and work distributions within a contact patch. The program has been modified to compute the creep moment distribution as well. These distributions, particularly the work distribution, are of interest in the conduct of wheel and rail wear investigations. The work distributions differ substantially from the parabolic distributions that we have assumed in earlier work.

Several three-dimensional plots for the distribution of creep force, creep moment, slip, spin and work done have been presented for typical cases of wheel/rail rolling contact. These plots help to visualize the force, slip, and work distributions within the contact patch.

A series of plots shows how the slip and adhesion regions depend upon various combinations of longitudinal, lateral, and spin creepage.

Acknowledgments

We appreciate the helpful suggestions made by the reviewers of this paper.

References

Carter, F. W., 1926, "On the Action of A Locomotive Driving Wheel," *Proceedings Royal Society*, A(112), pp. 151-157.

Fries, R. H., and Davila, C. G., 1987, "Wheel Wear Predictions for Tangent Track Running," ASME *Journal of Dynamic Systems, Measurement and Control*, Vol. 109, pp. 397-404.

Garg, V. K., and Dukipati, R. V., 1984, *Dynamics of Railway Vehicle Systems*, Academic Press.

Johnson, K. L., 1985, *Contact Mechanics*, Cambridge University Press.

Kalker, J. J., 1967a, "A Strip Theory for Rolling with Slip and Spin," *Proceedings KNAW*, B70, pp. 10-62.

Kalker, J. J., 1967b, "On the Rolling Contact of Two Elastic Bodies in the Presence of Dry Friction," Ph.D. dissertation, Delft University of Technology, Delft, Netherlands.

Kalker, J. J., 1967c, "On the Rolling Contact of Two Elastic Bodies in the Presence of Dry Friction: Numerical Results," Delft University of Technology, Delft, Netherlands.

Kalker, J. J. 1979, "Survey of Wheel-Rail Contact Theory," *Vehicle System Dynamics*, Vol. 5, pp. 317-358.

Kalker, J. J., 1982, "A Fast Algorithm for the Simplified Theory of Rolling Contact," *Vehicle System Dynamics*, Vol. 11, pp. 1-13.

Shen, Z. Y., Hedrick, J. K., and Elkins, J. A., 1983, "A Comparison of Alternative Creep Force Models for Rail Vehicle Dynamics Analysis," *The Dynamics of Vehicles on Roads and on Tracks: Proceedings of 8th IAVSD Symposium*, Cambridge, MA, p. 591-605.

Vermeulen, P. J., and Johnson, K. L., 1964, "Contact of Non-Spherical Elastic Bodies Transmitting Tangential Forces," ASME *Journal of Applied Mechanics*, Vol. 31, pp. 338-340.

Wang, B.-T., 1988, "A Computational Approach to the Prediction of Wheel Wear Profiles," M.S. thesis, Department of Mechanical Engineering, Virginia Polytechnic Institute and State University.